

Evidence of hexatic phase formation in two-dimensional Lennard-Jones binary arrays

Mo Li

*W. M. Keck Laboratory, Mail Stop 138-78, California Institute of Technology, Pasadena, California 91125
and Molecular and Materials Process Center, Beckman Institute, Mail Stop 139-72 California Institute of Technology,
Pasadena, California 91125*

William L. Johnson

W. M. Keck Laboratory, Mail Stop 138-78, California Institute of Technology, Pasadena, California 91125

William A. Goddard III

*Molecular and Materials Process Center, Beckman Institute, Mail Stop 139-72, California Institute of Technology,
Pasadena, California 91125*

(Received 22 April 1996)

We report evidence of the hexatic phase formation in Lennard-Jones binary substitutional random arrays from isothermal-isobaric molecular-dynamics simulations. The hexatic phase is analogous to those predicted in Kosterlitz-Thouless theory of melting that is characterized by short-range translational order and quasi-long-range orientational order. At the crystal to hexatic phase transition, dislocation pairs are observed to unbind into isolated dislocations. Further disordering of the hexatic phase, however, does not lead to dissociation of dislocations into disclinations. Instead, the dislocations become clustered and form dislocation networks which results in formation of amorphous phases. [S0163-1829(96)02741-5]

Melting in three dimensions is known to be a first-order transition where the sharp Bragg peaks of the crystalline phases abruptly become flat and smeared out. In two dimensions (2D), the long-range translational order of a crystalline phase is destroyed spontaneously by fluctuations of long-wavelength phonon modes, leaving it with quasi-long-range translational order (power-law decaying).¹ It was proposed by Kosterlitz and Thouless² (KT) that melting in two dimensions is a topological order-to-disorder transition that proceeds via dislocation pair unbinding. According to this theory, the liquid phase is a phase containing a certain fraction of isolated dislocations. Further analysis suggested that isolated dislocations alone can indeed destroy the quasi-long-range translational order in 2D crystalline phases, but leaves the long-range bond-orientational order intact.³ Therefore, the liquid phase defined by Kosterlitz and Thouless² has short-range translational order and quasi-long-range orientational order. According to Nelson and Halperin (NH),³ it is a liquid-crystal-like phase, the hexatic phase. The true liquid phase having short-range translational and orientational order forms when the isolated dislocations in the hexatic phase further unbind to form isolated disclinations. Therefore, it is possible for 2D crystalline phases to melt continuously via such two consecutive defect-unbinding processes involving an intermediate hexatic phase.

The defect-unbinding theory for 2D melting²⁻⁴ has drawn enormous attention in the past decade.⁵⁻⁷ The hexatic phase has been found in liquid crystalline phases, Coulomb gases, and vector dislocation models.^{5,8} However, it has long been debated whether hexatic phase exists for systems made of atoms interacting with pair-wise interactions such as hard sphere and Lennard-Jones (LJ) potentials.⁵⁻⁹ The consensus, largely due to extensive computer simulations in the past decade, is that the hexatic phase is unlikely to exist in these

systems.^{5-8,10,11} These studies have shown that dislocation densities increase precipitously during heating and more complex defects such as grain boundaries and dislocation aggregates usually form at the elevated temperatures. These results seem to contradict the theory of 2D melting which assumes that dislocations are relatively sparse and that at melting, dislocation pairs unbind to form simpler, more elementary defects such as isolated dislocations and disclinations. To mimic the conditions under which the hexatic phase is expected, more repulsive interatomic potentials⁶ have been used. But only in the case where the dislocation core energy is explicitly manipulated in a dislocation vector model have formation of hexatic phases been observed unambiguously.¹²

In this work, we chose a different path to study the hexatic phase formation by introducing disorder to a 2D crystalline phase. First, instead of heating it, we choose to alloy two types of atoms by mixing one into another under constant pressure and temperature. A similar procedure was taken by Nelson, Robinstein, and Spaepen¹³ to investigate bond-orientational order in binary arrays made of steel balls. In this experiment, larger balls of two different sizes were introduced into the matrix of smaller ones. The equilibrating and temperature effects were simulated by mechanically vibrating a flat tray containing the mixture of balls. They found that dislocations were created around the bigger balls when their nearest-neighbor coordinates deviate from those of the hexagonal lattice. At higher concentrations of the bigger balls, the hexatic phases as characterized by quasi-long-range orientational order and short-range translational order were reported to form.

With molecular-dynamics (MD) simulations, we can systematically investigate topological order and thermodynamic properties for binary arrays made of atoms interacting with

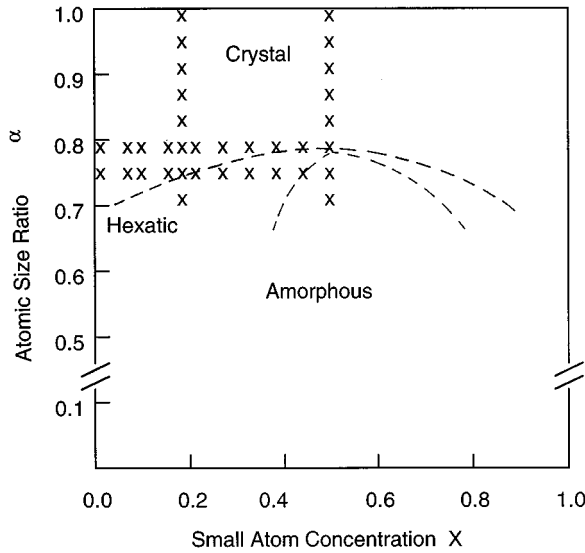


FIG. 1. Phase diagram in parameter space (α, x) at $T=0.2$ ($<T_g=0.22$) and $P=0.0$ for the 2D LJ binary arrays. X marks the phases simulated using MD.

realistic interatomic potentials. The binary arrays to be studied are made of atoms interacting with Lennard-Jones potentials,

$$\phi_{\alpha\beta}(r) = -4\epsilon_{\alpha\beta} \left[\left(\frac{\sigma_{\alpha\beta}}{r} \right)^{12} - \left(\frac{\sigma_{\alpha\beta}}{r} \right)^6 \right] S(r), \quad (1)$$

where α and β denote the two atomic species, A and B . $S(r)$ is the cubic spline switch function defined as

$$S(r) = \begin{cases} 1, & r \leq r_1 \\ 1 - \frac{(r-r_1)^2(3r_c-r_1-2r)}{(r_c-r_1)^3}, & r_1 < r < r_c \\ 0, & r \geq r_c \end{cases}$$

where $r_c=2.45\sigma$ and $r_1=1.90\sigma$ are the cutoff distance and the distance at which $S(r)$ is switched on, respectively. σ is the LJ parameter defined below. $S(r)$ is used to ensure smoothness of the potentials at the cutoff distances and to reduce statistical errors for long simulations.¹⁴

The two types of atoms are chosen such that they differ only in sizes. This is achieved by introducing the atomic size ratio, $\alpha=R_B/R_A$, where R_A and R_B are the atomic radii of the two types of atoms, A and B . For the LJ binary array, $\alpha=\sigma_{BB}/\sigma_{AA}$, where σ_{BB} and $\sigma_{AA}=\sigma$ are the parameters for A - A and B - B interatomic LJ potentials. Furthermore, the depths of the LJ potentials, ϵ_{AA} , ϵ_{AB} , and ϵ_{BB} , are set equal to ϵ in order to avoid chemical short-range ordering or clustering resulting from differences in those parameters. For the interaction between A and B atoms, we take $\sigma_{AB}=(\sigma_{AA}+\sigma_{BB})/2$. At given pressure and temperature, the binary array is therefore completely specified by only two parameters, the atomic size ratio α which is determined by the relative sizes of the two types of atoms and the relative concentration of the mixture $x=N_B/(N_A+N_B)$. Here N_A and N_B are the numbers of A and B types of atoms in the array.

Defects in the binary array are generated primarily by atomic size difference. Since the hexagonal lattice is the only

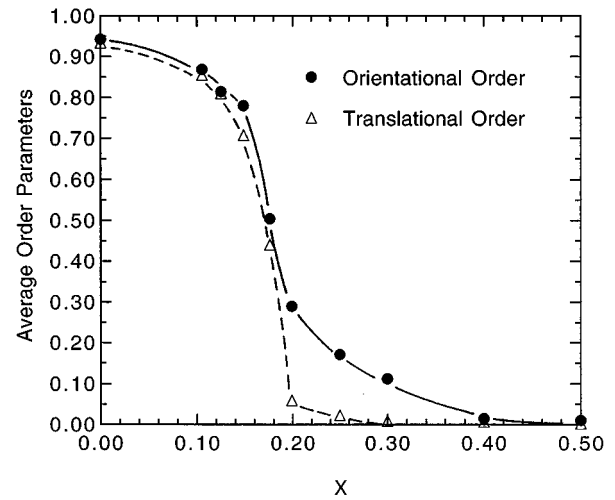


FIG. 2. Average translational and orientational order parameters. The former is defined as $(1/N)\sum_i^N \rho_G(r_i)$, where $\rho_G(r_i) = \exp[i\mathbf{G}\cdot\mathbf{r}_i]$. The latter is defined as $(1/N)\sum_i^N \Psi(r_i)$ (Ref. 23), where $\Psi(r_i) = (1/N_{NN})\sum_j^{N_{NN}} \psi_6(r_{ij})$, and $\psi_6(r_{ij}) = \exp[im\theta(r_{ij})]$, where $m=6$. N_{NN} is the number of the nearest neighbors of atom i and $\theta(r_{ij})$ is the angle of the nearest-neighbor bond i - j with respect to the reference axis.

close-packed, lowest energy configuration in 2D, substitution with solute, or impurity atoms, with different atomic size introduces disparity to the local packing in the host crystalline lattice.¹⁵ This size difference causes changes in interatomic interactions among the atoms within the potential cut-offs. After relaxation, it leads to local distortion in atomic positions and strain fields on the lattice, both of which contribute to increase of free energies of the disordered binary arrays. As more and more solute atoms are introduced, distortions become more acute and the crystalline lattice becomes softer. Eventually, under the combined effects of temperature (atom vibration) and the lattice softening, the local sixfold symmetry of the atoms with nearest neighbors of different sizes is broken and disclinations are generated. As shown below, the binary arrays with the simplest choice of interatomic potential parameters can have the same topological defects as those in a pure LJ solid at melting.

Compared with the monoatomic systems, the binary arrays have an additional degree of freedom, x , that we can utilize to avoid defect clustering which is a direct competing process with defect unbinding. The alloying process takes place while the binary mixtures are kept at constant temperatures below the glass transition temperature T_g . Here T_g is determined previously by quenching the corresponding binary liquids using constant pressure MD with quench rate of 10^9 K/s. At such low temperature, it is difficult for defects to aggregate through long-range diffusion. The defects, once generated, are then pinned, or frozen. Therefore, by alloying two different types of atoms, we have possibilities to observe hexatic phase formation and crystal to amorphization transition by traversing the crystal-hexatic phase boundary as we change the relative atom concentration x at constant temperature.

Starting from a pure LJ crystal made of bigger atoms on the hexagonal lattice, we prepared the substitutional arrays by either randomly replacing them by the smaller ones with

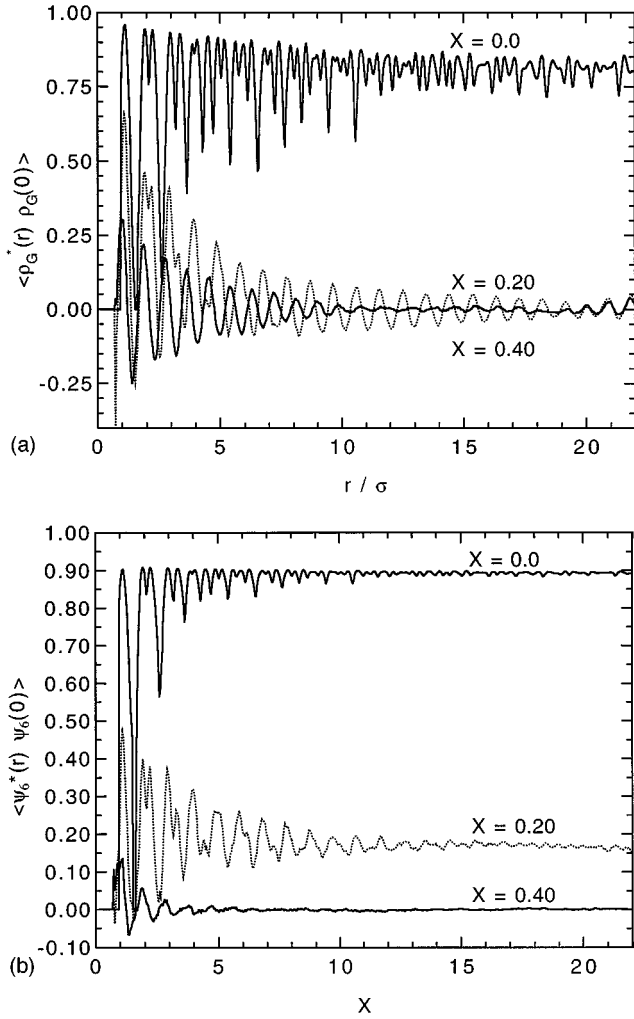


FIG. 3. (a) Translational order correlation function $\langle \rho_{G(r)}^* \rho_G(0) \rangle$ and (b) orientational order correlation function $\langle \psi_6^*(r) \psi_6(0) \rangle$ for LJ binary arrays with 1764 atoms.

the relative concentration x at each given atomic size ratio α , or by varying α of the binary mixtures at a given x . We used both methods for samples made of 1024, 1764, 2500, and 10^4 atoms and found no significant difference in the results.

Thermodynamic and structural properties of the binary substitutional random arrays were obtained using constant pressure and temperature MD methods.^{16,17} Technical details for the simulations can be found in Ref. 17. Here, we only briefly mention some additional procedures unique for the binary arrays. First, a relatively long simulation time is needed for equilibration since the arrays are at low temperature. It usually takes about 10^5 MD steps for each array. When the arrays are close to the hexatic phase boundary, it was necessary to carry out extremely long simulations (up to 10^7 MD time steps) to obtain thermodynamic properties. Second, we performed configuration averages on the thermodynamic properties, in addition to the time averages. About 5–10 different configurations of binary array that have different initial random distributions of small atoms were used for the configuration averages.

In the following, we present our results using isothermal and isobaric MD simulations of the binary arrays with $\alpha=0.75$ at $T=0.20$ (in reduced LJ units) and $P=0.0$. T_g is

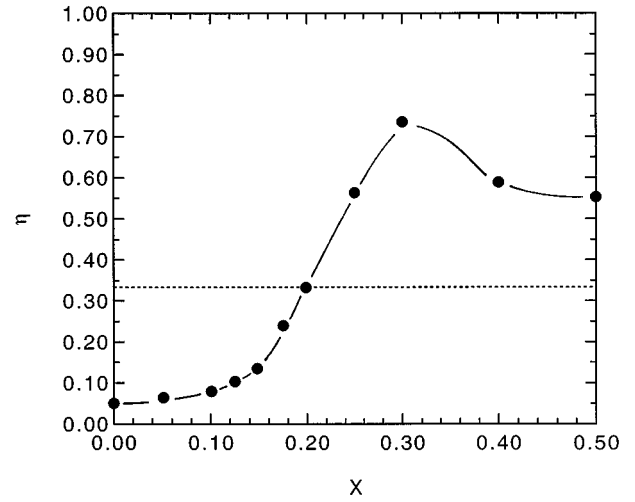


FIG. 4. The exponent of the algebraic decaying translational order correlation function determined using Eq. (2).

about 0.22 for these arrays. Results for other systems with different size ratios are summarized briefly in Fig. 1. As shown in the phase diagram, there are three distinctive phases in the 2D binary arrays in different regions when $\alpha < \alpha_c = 0.82$, crystalline, hexatic, and amorphous. They are characterized by different translational and orientational order. As shown in Fig. 2, the average translational and orientational order parameters for those arrays with $\alpha=0.75$ show three regions corresponding to the three different phases. The hexatic region begins at $x \approx 0.20$ where the translational order parameter is almost zero, but the orientational order parameter is still finite. At higher concentrations, one observes slow decrease of the bond orientational order. At $x \geq 0.40$, both order parameters become nearly zero.

As shown in Fig. 3(a), the translational order correlation functions in the pure LJ solid decay algebraically with distance. This quasi-long-range order in translational symmetry is due to fluctuations in long-wavelength phonon modes.¹⁻³ In contrast, the orientational order correlation function remains a constant close to unity as predicted in the theory of

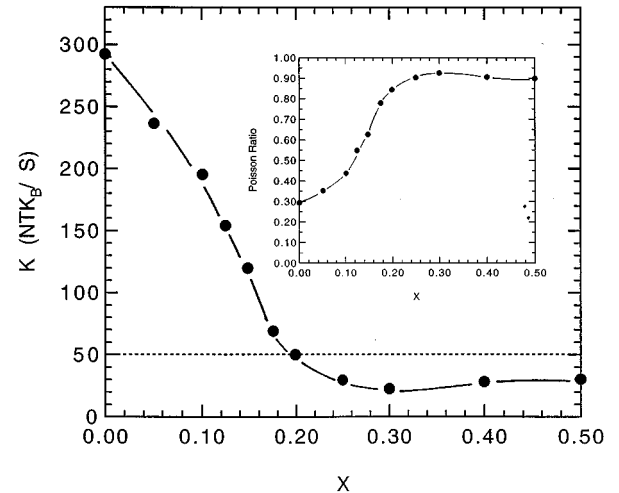


FIG. 5. The Kosterlitz-Thouless constant. S is the total area of the 2D arrays. The dotted line is 16π . The inset is the Poisson ratio.

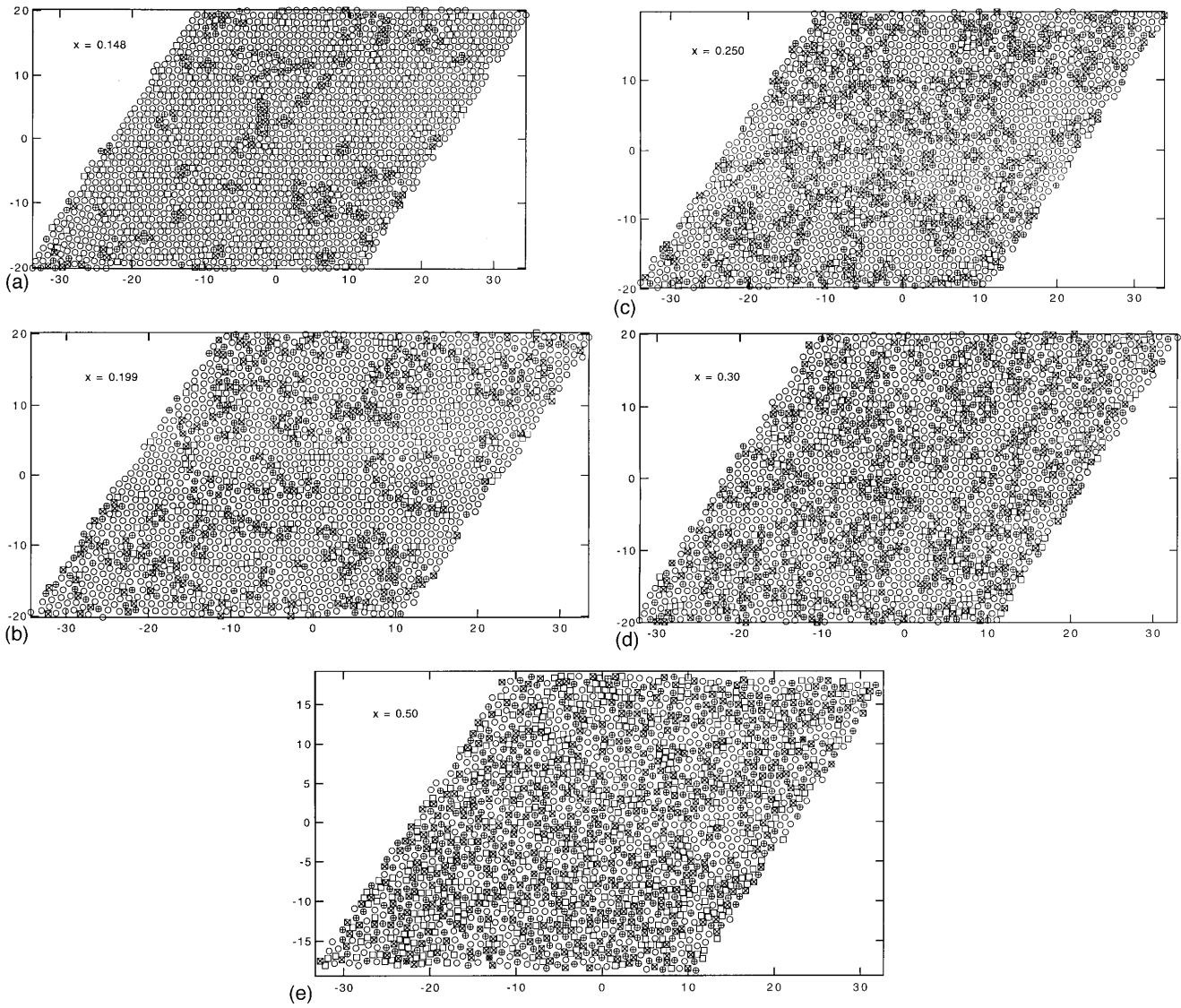


FIG. 6. Atomic configurations of defects at (a) $x=0.15$, (b) $x=0.20$, (c) $x=0.25$, (d) $x=0.30$, and (e) $x=0.50$. The crosses denote five nearest-neighbor (NN) disclinations, the plus signs are 7NN ones, and the asterisks are 8NN ones. A 5NN disclination and a nearest-neighbor 7NN disclination form an edge dislocation (Ref. 18). The bigger atoms are represented as circles and smaller atoms as squares.

2D melting.³ As shown in Fig. 3(b), it becomes algebraically decaying once the B atoms are alloyed into the matrix of A atoms. At the hexatic phase boundary ($x \approx 0.20$), the correlation function of translational order parameters decays to zero at a distance approximately close to the fourth-nearest neighbors; while the orientational order correlation function still remains quasi-long-range. The latter remains finite until x reaches 0.4 where both order correlation functions become short ranged.

As predicted by the theory of 2D melting the power-law decay of the translational correlation of the crystalline solid phase, $\rho_G(r) \sim r^{-\eta_G}$, has an exponent η_G that cannot exceed $1/3$.³ Indeed, our results show that it approaches this limiting value as the hexatic phase boundary is reached (Fig. 4). The exponents can be obtained by either fitting the correlation functions $\rho_G(r)$ or using the result³

$$\eta_G = \frac{|\mathbf{G}|^2 k_B T}{4\pi} \frac{3\mu + \lambda}{\mu(2\mu + \lambda)}, \quad (2)$$

where μ and λ are the Lamé constants that are related to the isothermal elastic constants. The elastic constants are calculated directly in our simulations by utilizing fluctuations of the MD cell shape.^{16,17} \mathbf{G} is the shortest reciprocal-lattice vector in the hexagonal lattice. As shown in Fig. 3(b), the correlation functions for the bond-orientational order parameters decays as $\rho_6(r) \sim r^{-\eta_6}$ with exponents, η_6 , that remain below the limiting value $1/4$ (Ref. 3) for $x < 0.40$ in the hexatic phase before the amorphous phase forms.

Thus far, the results presented above suggest that the transition at $x \approx 0.20$ leads to a hexatic amorphous phase. As proposed in the KTNHY theory,^{2,3} it should involve dislocation pair unbinding to form a certain fraction of isolated dislocations. Such a process can be measured by the dislocation coupling constant, or the Kosterlitz-Thouless constant,²

$$K = \frac{4a^2}{k_B T} \frac{\mu(\mu + \lambda)}{(2\mu + \lambda)}, \quad (3)$$

where a is the lattice parameter. At the transition, K should approach an universal constant, 16π , due to screening effects on the shear elastic modulus from presence of other dislocations.³ Figure 5 shows the dislocation coupling constant versus concentration at $\alpha=0.75$ calculated using Eq. (3). At the transition, one sees clearly that K approaches this value within 5% of the standard deviations.¹⁷ It levels off in the hexatic phase and becomes almost flat in the amorphous phase. In contrast, it becomes zero immediately at melting.³

Additional evidence for the formation of the hexatic phase is from visual observations of the atomic configurations of defects. Such observations however, can be misleading if the conditions of the observation are not specified clearly. For example, an evolving atomic configuration during a phase transition can be mistaken as the equilibrium configuration of a new phase if one does not specify the time span of the snapshot. In our work, we mapped out the configurations of dislocations and disclinations using nearest-neighbor coordinates.¹⁸ This is usually done using Voronoi polyhedron construction. In a binary array with large atomic size difference, the Voronoi technique is not reliable. Instead, we used Fisher and Kock's radical plane method¹⁹ to locate the nearest neighbors for atoms with different sizes. Figure 6 shows snapshots of some typical atomic configurations for various defects at $x\approx 0.15, 0.20, 0.25, 0.30,$ and 0.50 . Since the arrays are kept at low temperature, these configurations do not show large changes in the period of a few thousand MD steps after equilibration. In the crystalline phase ($x\leq 0.15$), we find that dislocations are tightly bond into pairs with only a neglectable number of isolated disclinations or dislocations. For $x>0.15$, the number of dislocations increases slowly at first and then rises precipitously. Correspondingly, the defect configuration exhibits quantitative changes. As shown in Fig. 6, at $x=0.20$, the dislocations become more diffuse and seem to be breaking loose as compared with the tightly bonded pairs in the crystalline phases. Defining isolated dislocations to be the ones that are at least one lattice parameter apart, we can see that about 15% of the dislocations are in isolated state at the hexatic phase transition. The rest of dislocations are still paired, but they are more loosely bonded and become elongated, or stretched. As the concentration of small atoms increases, both isolated and paired dislocations tend to form chainlike small segments. Many of those chainlike segments are made of several elongated dislocation pairs, making it difficult to determine if they are still dislocation pairs [see Figs. 6(c) and 6(d)]. As disordering increases with increasing concentration x , we observed neither that the isolated dislocations are dissociated into isolated disclinations nor that the dislocation pairs further unbind to form isolated dislocations. Instead, they tend

to form network chain, or grain-boundary-like configurations first and become clustered later, as shown in Figs. 6(d) and 6(e). This trend continues until the amorphous phase forms. It appears that the hexatic phase "melts" and becomes an amorphous phase when the dislocation network chains, or grain-boundary-like defect complexes proliferate. Chui¹¹ in his grain-boundary-mediated melting theory predicted such a phenomenon. But he predicted a much sharper transition than the one we observed here.

We also observed a first-order "melting," or "amorphization," at the equimolar concentration $x=0.5$ upon varying α .²¹ This is in agreement with the early report by Bocquet *et al.*²⁰ The transition at this point is abrupt with changes in both order parameters and also in enthalpy and volume. In contrast, the amorphization involving the hexatic phase is continuous in all the properties. From the phase diagram (Fig. 1) we see that the hexatic phase region gradually closes when the atomic size difference becomes smaller and as the smaller atoms are more concentrated. In addition, we found that the transition become more abrupt at elevated temperatures above T_g .²¹ At low temperature ($T<0.15$), we found that dislocation unbinding becomes very difficult because of the increase in shear elastic constant. The latter leads directly to increase in the dislocation coupling constant, K . The transition becomes very sluggish, almost losing the characteristics of a phase transition.²¹ A recent study of a 2D crystal subjected to a slowly varying random potential suggests that there could exist KT transitions even down to zero temperature.²² The apparent inconsistency between our results and the theory may result from slow kinetics of the transition in our simulations.

In conclusion, we found evidence of the hexatic phase formation in the diffusionless, random binary arrays by "alloying" or mixing two types of atoms of different sizes. The hexatic phase is characterized by the quasi-long-range orientational order and short-range translational order. We found that the hexatic amorphous phase forms when a certain fraction of dislocation pairs unbind to become isolated. The ordering and thermodynamic properties of the hexatic phase forming binary arrays bear striking similarities with those predicted in the theory of 2D melting.^{2,3} However, we found that further disordering of the hexatic amorphous phase does not lead to dislocation unbinding. Instead, we observed that dislocations tend to cluster and form network chains or grain boundaries, which appears to be the underlying mechanism for formation of amorphous phases.

We would like to thank D. Webb and P. B. Weichman for many stimulating discussions. This work is partially supported by the Department of Energy (Grant No. DE-FG03-86ER45242).

¹L. D. Landau and E. M. Lifshitz, *Statistical Physics*, 2nd ed. (Pergamon, Oxford, 1980); N. D. Mermin, *Phys. Rev.* **176**, 250 (1968).

²L. M. Kosterlitz and D. J. Thouless, *J. Phys. C* **6**, 1181 (1973).

³D. R. Nelson and Halperin, *Phys. Rev. B* **19**, 2457 (1979).

⁴A. P. Young, *Phys. Rev. B* **19**, 1855 (1979).

⁵F. F. Abraham, *Phys. Rep.* **80**, 339 (1980).

⁶K. J. Strandburg, *Rev. Mod. Phys.* **60**, 161 (1988).

⁷M. A. Glaser and N. A. Clark, *Adv. Chem. Phys.* **83**, 543 (1993).

⁸For a recent review, see *Bond Orientational Order in Condensed Matter Systems*, edited by K. J. Strandburg (Springer-Verlag, New York, 1992).

⁹K. Chen, T. Kaplan, and M. Mostoller, *Phys. Rev. Lett.* **74**, 4019 (1995).

- ¹⁰W. Janke and H. Kleinert, *Phys. Lett. A* **105**, 134 (1984).
- ¹¹S. T. Chui, *Phys. Rev. B* **28**, 178 (1979).
- ¹²Y. Saito, *Phys. Rev. B* **26**, 6239 (1982).
- ¹³D. R. Nelson, M. Robinstein, and F. Spaepen, *Philos. Mag. A* **46**, 105 (1982).
- ¹⁴F. H. Stinlinger and A. Rahman, *J. Chem. Phys.* **57**, 1281 (1972).
- ¹⁵F. Spaepen, *J. Non-Cryst. Solids* **31**, 207 (1978).
- ¹⁶M. Parrinello and A. Rahman, *Phys. Rev. Lett.* **45**, 1196 (1980).
- ¹⁷M. Li and W. L. Johnson, *Phys. Rev. B* **46**, 5237 (1992).
- ¹⁸A. McTague, D. Frenkel, and M. P. Allen, in *Ordering in Two Dimensions*, edited by S. K. Sinha (North-Holland, Amsterdam, 1980).
- ¹⁹W. Fisher and E. Kock, *Z. Kristollogr.* **150**, 245 (1979).
- ²⁰L. Bocquet, L-P. Hansen, T. Biben, and P. Madden, *J. Phys. Condens. Matter* **4**, 2375 (1992).
- ²¹M. Li, W. L. Johnson, and W. A. Goddard (unpublished).
- ²²M. C. Cha and H. A. Fertig, *Phys. Rev. Lett.* **74**, 4867 (1995).
- ²³K. J. Strandburg, J. A. Zollweg, and G. V. Chester, *Phys. Rev. B* **30**, 2755 (1984).